Excerpts from Report of

Project MICHIGAN

Infrared Detector Research (U)

Period 1 October 1954 to 1 March 1955

Contract No. DA-36-039-SC-52654

DA Project No. 3-99-10-024

Signal C No. 102 D

Placed by
CHIEF SIGNAL OFFICER
Department of the Army

2144-40-P

Vol. II

The University of Michigan
Engineering Research Institute
Willow Run Research Center
Willow Run Airport
Ypsilanti, Michigan

3.2 DETECTOR RESEARCH

Photon detectors have been of practical value since the discovery of the photoelectric effect. Each photoelectric material, however, has a long wavelength limit of sensitivity, determined by its work function, which seldom exceeds one micron. In order to detect photons of longer wavelengths, and hence lower energy, attention turned to processes of photoconductivity. We should mention here the work of G. W. Hammer and co-workers of the Eastman Kodak Company leading to the Ektron PbS cells; of Levinstein on the photoconductivity of PbTe (Ref. 10); of Burstein, Morton and Dunlap on Ge and Si (Ref. 10). Recently attention has been drawn by Welker (Ref. 11) and Breckenridge (Ref. 12) to the semiconductor nature of 3-5 intermetallic compounds, so designated because they are comprised of elements which fall in the third and fifth columns of the periodic table. Study of these compounds has only begun, but we may mention the photoconductivity of InAs (Talley, Ref. 13) and the photovoltaic effect in InSb (Moss, Kurnick and Zitter (Ref. 10)). The intermetallic compounds show great promise for use as photoconductive and photovoltaic detectors in the infrared.

It is well known that most infrared photo-detectors are limited in their usefulness by a high noise level (Ref. 14). Since the quantum efficiency of the better photoconductive detectors is near unity in the spectral region where they respond, the useful sensitivity of the detector can be increased by reducing this noise level.

The program on detector research has as its objective the preparation of semiconducting materials, especially the 3-5 intermetallic compounds, and the study of their photoconductivity and noise properties. During the report period equipment for these purposes was designed and constructed and initial experiments began.

3.2.1 Purification of Material

The fundamental electrical properties of semiconducting materials are known to depend to a large extent on the nature and concentration of impurities embedded in the semiconducting material. Extremely small concentrations (1/1,000,000 to 1/1,000,000,000) are effective in making large changes in those properties. It is because of this hypersensitivity of semiconducting properties to impurity content that great care must be exercised in the purification process in order to obtain a final material whose properties would be both useful and reproducible. In addition, all impurities must be removed before any one impurity is added in controlled amounts to determine its effects.

Almost any change of state of a substance offers an opportunity to obtain a segregation of the impurities that are contained in it. One commonly used method is vacuum distillation which makes use of the change in state from liquid or solid to vapor. Another method known as zone melting (Ref. 15) makes use of the interconversion between solid and liquid. Still other methods involve the use of an auxiliary reagent such as the precipitation of a substance from a solution. The number of purification methods and combinations of methods one might use are certainly great. However, the methods of purification which are now most commonly used for semiconducting materials are vacuum distillation and zone melting. During the report period, a zone melting system was designed, constructed, and operated. Ingots of indium, antimony, indium antimonide, and aluminum antimonide were purified by this apparatus. Arrangements are being made for spectroscopic tests of the purity of these ingots.

Figure 6 shows a close-up view of the zone-melting apparatus. A specially prepared carbon boat is milled dry from a 12-inch spectroscopic carbon rod and then baked out at about 1400° C in a hydrogen atmosphere for several hours in order to vaporize any volatile impurities. A charge

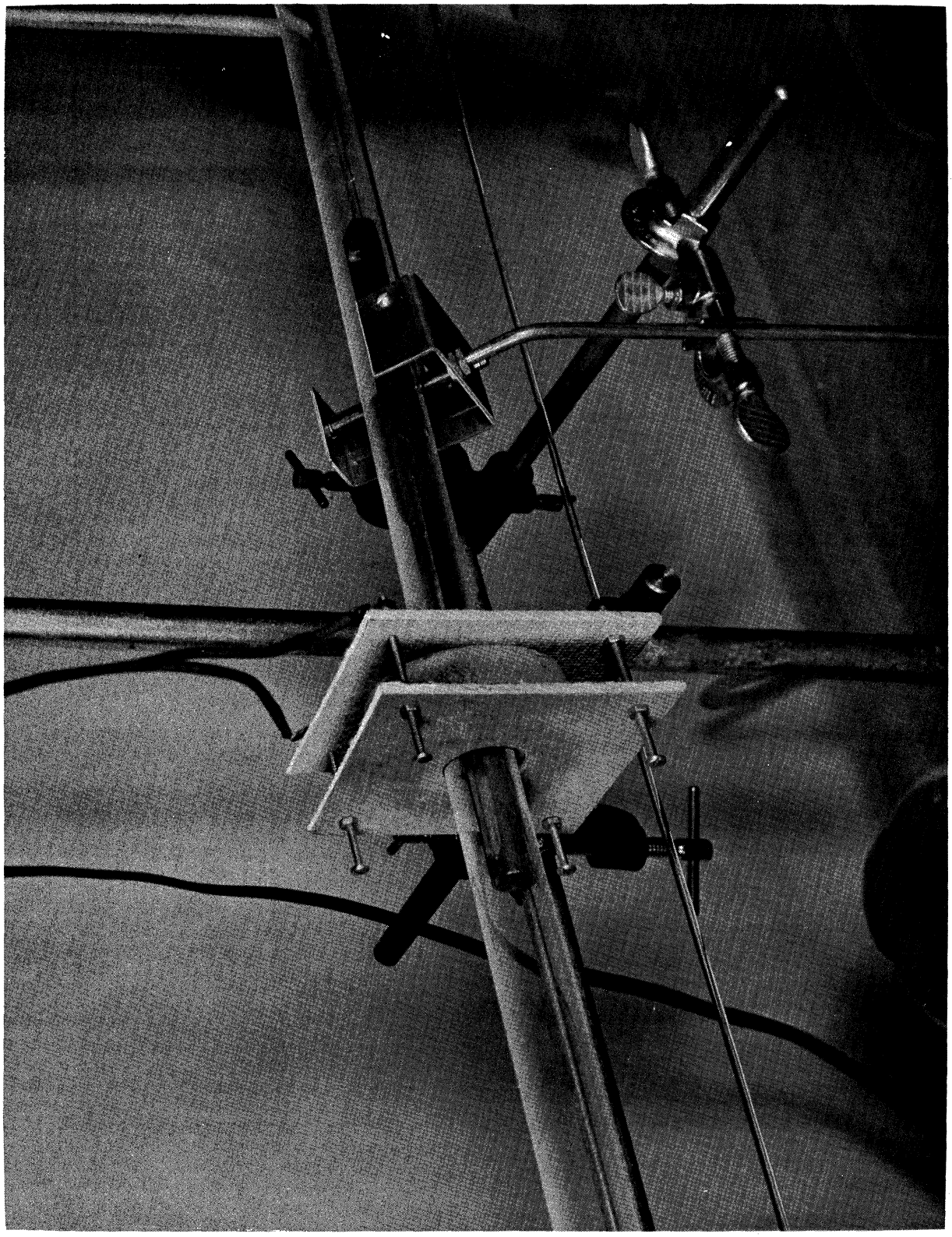

FIG. 6 CLOSE VIEW OF ZONE MELT APPARATUS

of 99.95 per cent pure indium metal is then melted down in the boat in a hydrogen atmosphere, and the oxide is slagged off with a pyrex glass hoe. After the slag has been removed and the metal has solidified into an ingot the zone melting process is begun at the left end (Fig. 6) by the narrow electric furnace. Just enough heat is supplied to maintain a molten zone one- to two-inches wide. The glass tube carrying the boat is moved through the furnace at a speed of one to eight inches per hour by a clock motor, so that the portion of the ingot moving into the furnace gradually melts. In this way a sharp molten zone moves relative to the ingot until the right end of the boat passes through the furnace.

The impurities in indium which tend to reduce the melting point will tend to stay in the molten zone and be carried toward the right end of the ingot; the impurities which tend to increase the melting point will tend to freeze out toward the left end of the ingot. With both types of impurities present both ends of the ingot will be less pure and the central portion more pure than the original ingot. By making a large number of zone melt passes, greater purity may be obtained in the central region, up to a limit depending upon the original purity of the material and the nature of the impurities. Further purification may be achieved by combining the central pure portions of two zone melted ingots to make a third ingot, on which the zone melt process can again be carried out.

Precautions must be taken to avoid contamination of the ingot by impurities contained in the gas above the ingot. For this reason the zone melting process is carried out either in a vacuum or in a purified gas atmosphere; the latter technique has been used in our work to date. The assembled equipment, including the gas lines, is shown in Figure 7. Two lines enter a small mixing tube at the upper right. One line is fed by purified hydrogen gas from which the last traces of oxygen have been removed by a De-Oxo unit. The other line is fed with helium gas. The two gases may be mixed in any proportion desired. The purpose of the hydrogen gas is to remove traces of oxygen from the helium gas during the passage of the mixture through a second De-Oxo unit. In some cases hydrogen gas is used alone; however, in the case of arsenides and phosphides large concentrations of hydrogen gas may combine with arsenic and phosphorus so that the ingot will no longer be stoichiometric. The water vapor which

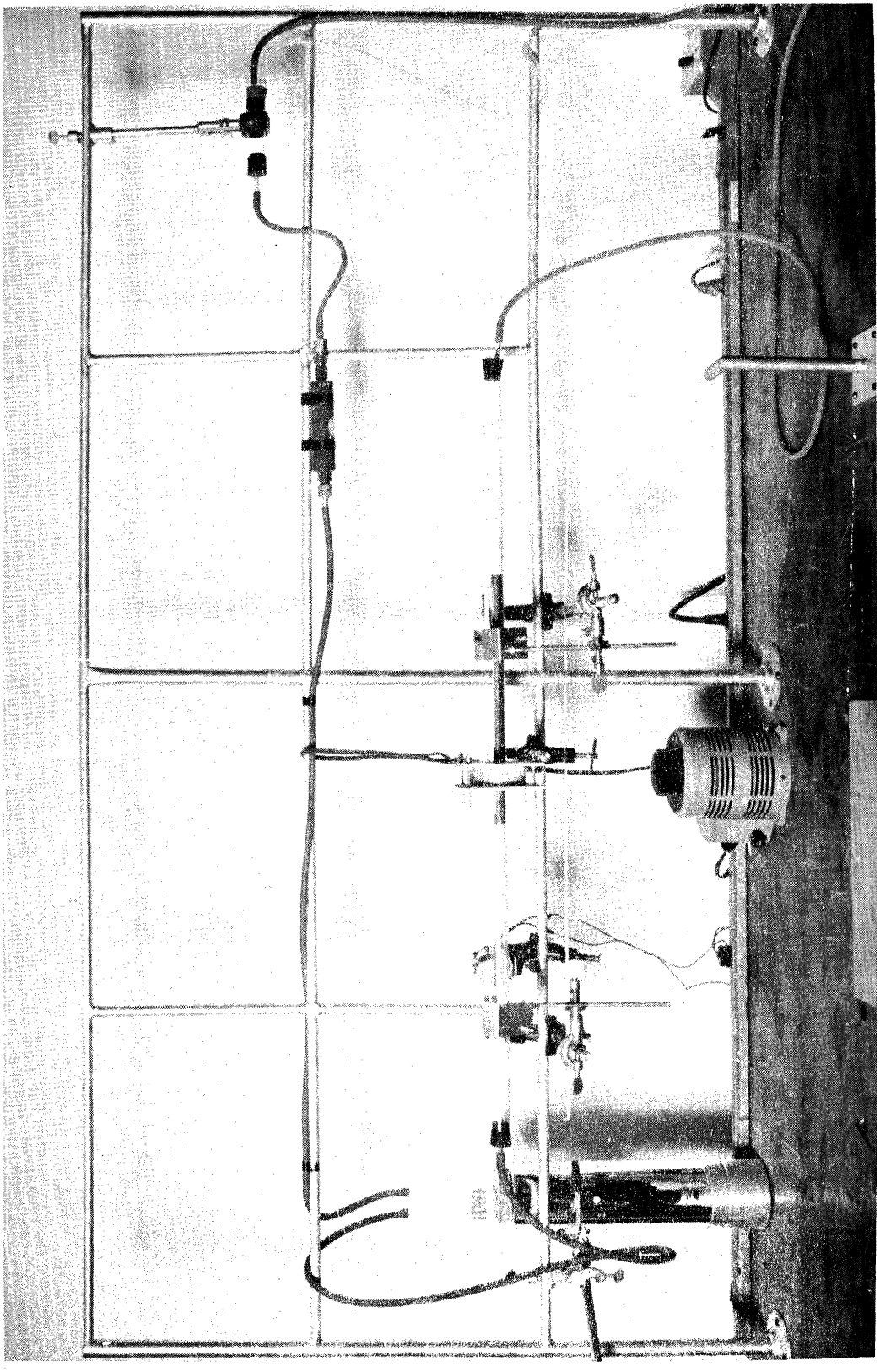

FIG. 7 VIEW OF ZONE MELT SYSTEM SHOWING GAS LINES

results from the combination of the hydrogen with the traces of oxygen is frozen out by passing the gas through a liquid air trap.

A closed circulating gas system is under contruction which will conserve the gases and avoid the replenishment of impurities which come from the supply tank. In conjunction with the closed gas system, three automatic zone melt units, one of which is shown in Figure 8, have been designed and constructed so that purification may proceed without attention. In these units a motor quickly and automatically returns the ingot to its starting position after each complete pass through the furnace.

3.2.2 Preparation of Single Crystals

The fundamental electrical properties of the semiconducting material are most easily studied on large single crystals of the highly purified material without grain boundaries. There are a number of methods for growing single crystals. In the self-seeding methods one endeavors to place a liquid or vapor in such an environment that only one or at most a few microcrystals form spontaneously at the beginning of the growing time and no new microcrystals are allowed to form thereafter. These initially formed microcrystals are called seeds. If several seeds are formed, one of them will usually grow faster than the others and may finally occupy the majority of the volume of the material. The one largest single crystal grain can then be cut out and separated from the rest. The artificial seeding methods make use of a small single crystal which one must have already on hand. This small single crystal then acts as a seed in the same growing process as described above. Growth of a single crystal is less critical by artificial seeding than by self-seeding because the physical conditions which allow one seed crystal to form spontaneously in the self-seeding method also may allow many others to form along with it.

A Kyropolous apparatus (Fig. 9 and 10) was constructed and set into operation during the report period; it utilizes an artificial seeding method, the procedure being as follows: A pure carbon crucible containing the zone-purified semiconducting material is placed on the ceramic stand seen in the lower central portions of the figures. The artificial (single) crystal seed, about 1 cm long and a few mm in diameter, is inserted in the stainless steel chuck above the crucible. A Vycor tube (not shown)

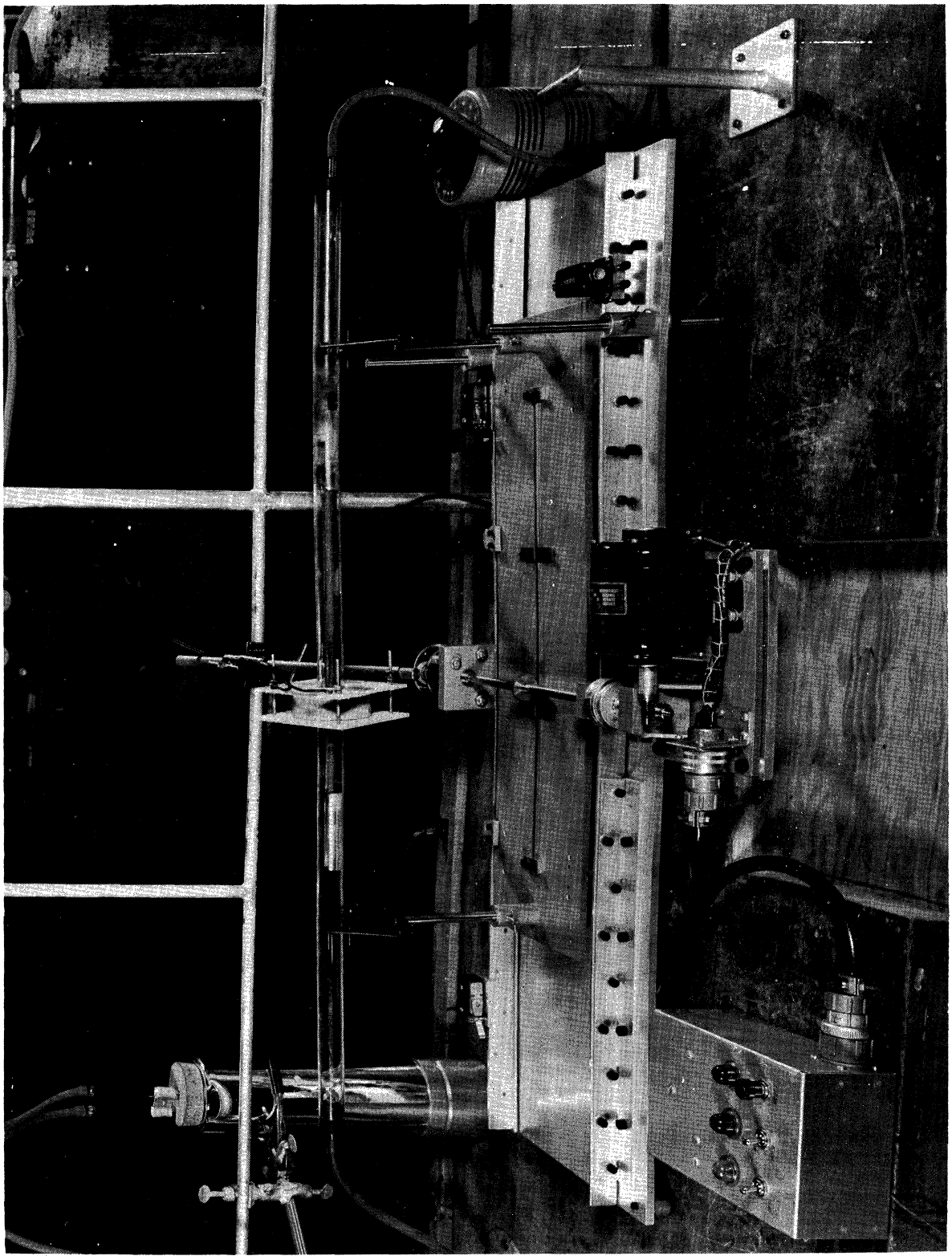

FIG. 8 AUTOMATIC ZONE MELT APPARATUS

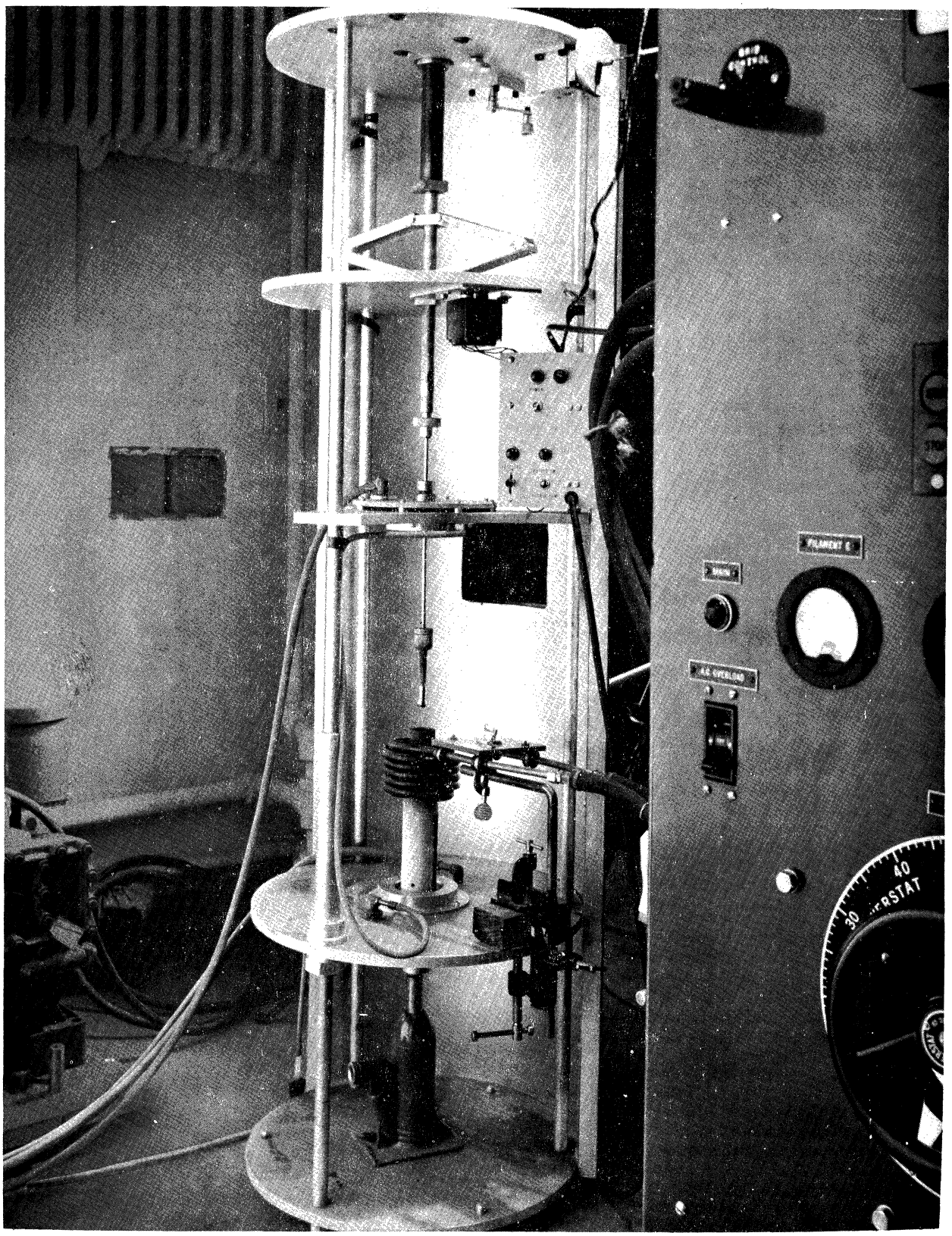

FIG. 9 KYROPOLOUS APPARATUS

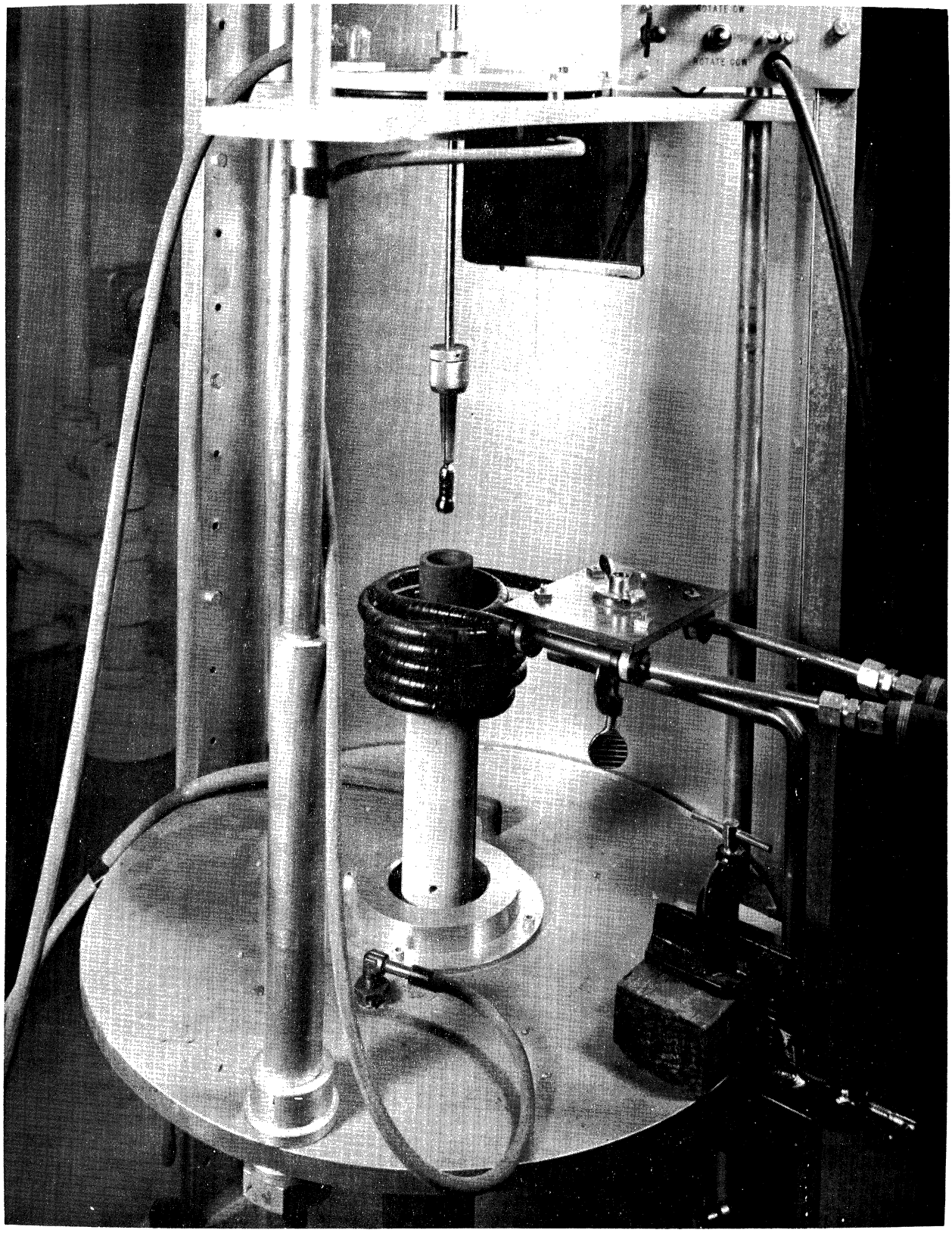

FIG. 10 CLOSE VIEW OF KYROPOLOUS

encloses the crucible and chuck and contains the inert or reducing atmosphere. A water-cooled coil of copper pipe which forms the induction heating coil is set around the outside of the glass tube. The material in the crucible is brought to the melting point and the seed crystal is brought into contact with the molten surface. As the seed crystal is slowly drawn up from the surface, the meniscus of the molten material freezes to the seed crystal so that the end of the seed gradually grows wider and longer. A resulting single crystal is shown in the chuck in Figure 10.

Two single crystals of nickel-doped germanium were grown so that the (100) axis lies along the direction of the pull. A third crystal was grown so that its (110) axis lies along the direction of pull. One of the largest single crystals grown here is shown in Figure 11. Figure 12 shows the appearance of the lower cut section after sandblasting. The polycrystalline nature of this portion, caused by excessively rapid freeze-out, is shown clearly in the oblique lighting. The cut section about 1 cm above is shown in Figure 13. Notice that no grain structure appears upon sandblasting; the slight shading at the lower left is a saw mark.

An attempt has been made to self-seed indium antimonide in the zone melt apparatus by using a boat with a sharp corner cut in one end; however, multiple seeding occurred so that a polycrystal ingot resulted.

3.2.3 Sample Preparation

In the preparation of the semiconducting sample for testing its optical and electrical properties, the important characteristics are the geometry and the surface treatment of the sample, and the nature of the electrical contacts.

Figure 14 shows a sample prepared for noise measurements in a manner similar to that used by Montgomery (Ref. 16). The two end contacts are used as current electrodes. The bar in the center is the material which is being tested. The side arms provide a means of applying potential measuring contacts without affecting the sample properties.

The samples are prepared by first cutting a thin disc from a single crystal boule (Fig. 11) with a diamond saw. Discs have been cut as thin

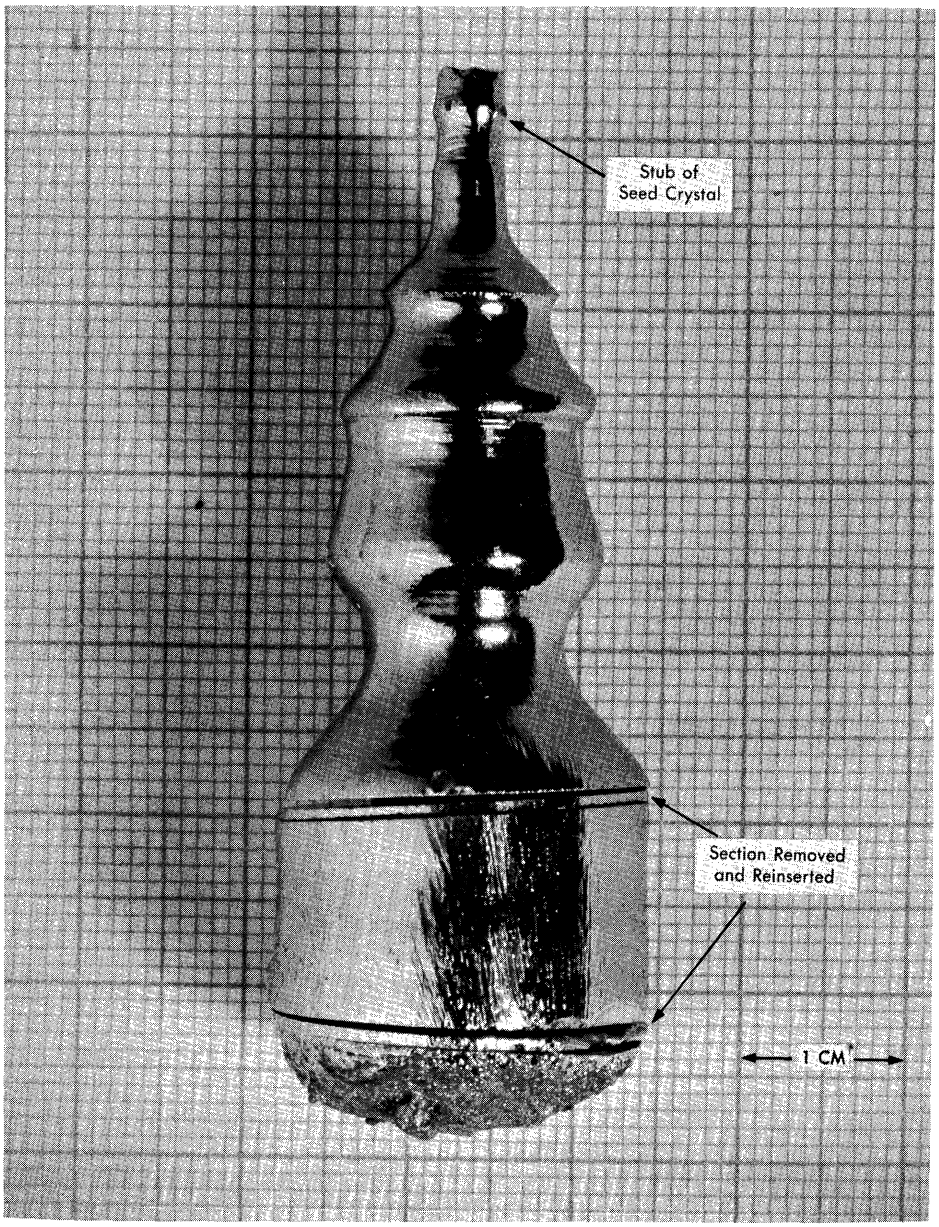

FIG. 11 SINGLE CRYSTAL BOULE OF NICKEL-DOPED GERMANIUM

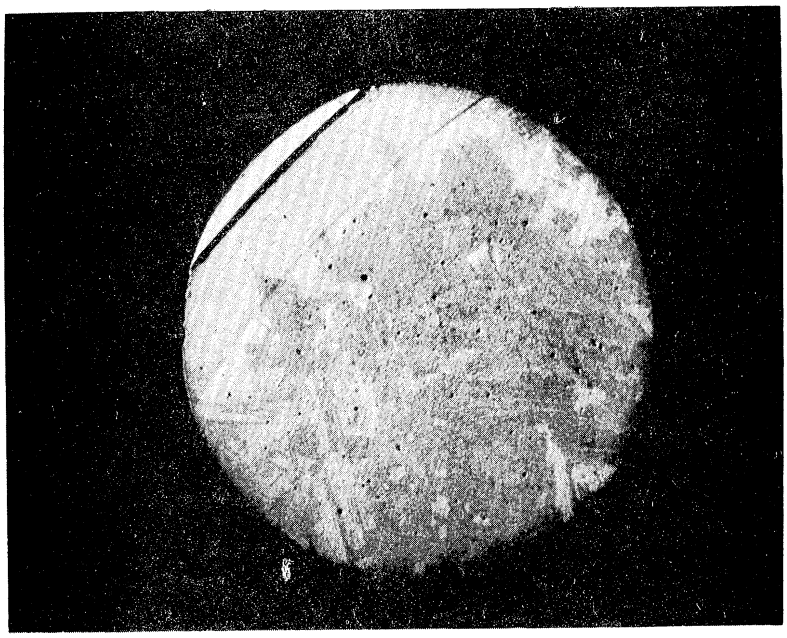

FIG. 12 POLYCRYSTALLINE SECTION

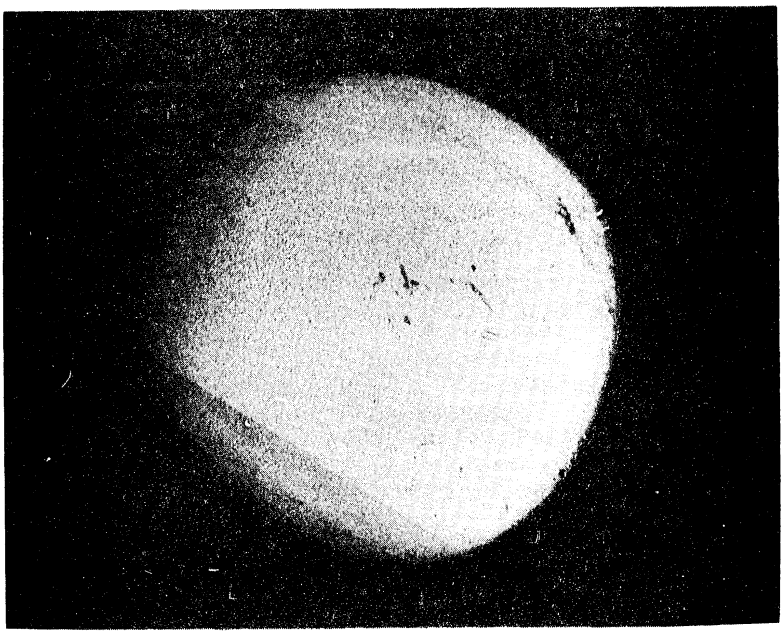

FIG. 13 SINGLE CRYSTAL SECTION

as 0.025 inches; thinnner sections are obtained by grinding. The multi-armed cross shape of Figure 14 is cut from the disc with a dust cutter mounted on a lathe tool mount and hood arrangement designed and constructed here during the report period (Fig. 15). The dust cutter head is an industrial abrasive unit made by S. S. White Dental Company. Very thin samples were mounted on a microscope slide cover before cutting. Two types of surface treatment were used--chemical etching and sand-blasting.

It is desirable to reduce or eliminate the effect of the contacts as possible noise sources. If one uses the geometry shown in Figure 14 with the side arms as potential electrodes, the only difficulties one would expect would be contact noise from the current electrodes and the possible injection of minority carriers from all electrodes.

The effect of contact noise will be minimized by using a constant-current source. Injection of minority carriers is minimized by using special solder and soldering techniques, using large-area contacts, and sandblasting the arms connecting the contacts to the sample so as to reduce the lifetime of the injected minority carriers. The solder is made to diffuse into the contact arms by heating in a hydrogen atmosphere at about 450° C. Figure 16 shows the bell jar and heating element arrangement used during this process. During the report period six samples of single crystal germanium were prepared for electrical measurements in this way.

3.2.4 Electrical and Optical Measurements

As stated previously the major aim of this program is to study the photoconductive and noise properties of semiconductors. These properties must be correlated with other basic properties such as Hall coefficient, dark conductivity, bulk and actual lifetime, and infrared transmission.

The major pieces of laboratory equipment needed for the measurement of these basic properties are a double monochromator for a source of monochromatic light, a black-body radiator for calibration purposes, a calibrated electromagnet to supply a uniform and variable strength field,

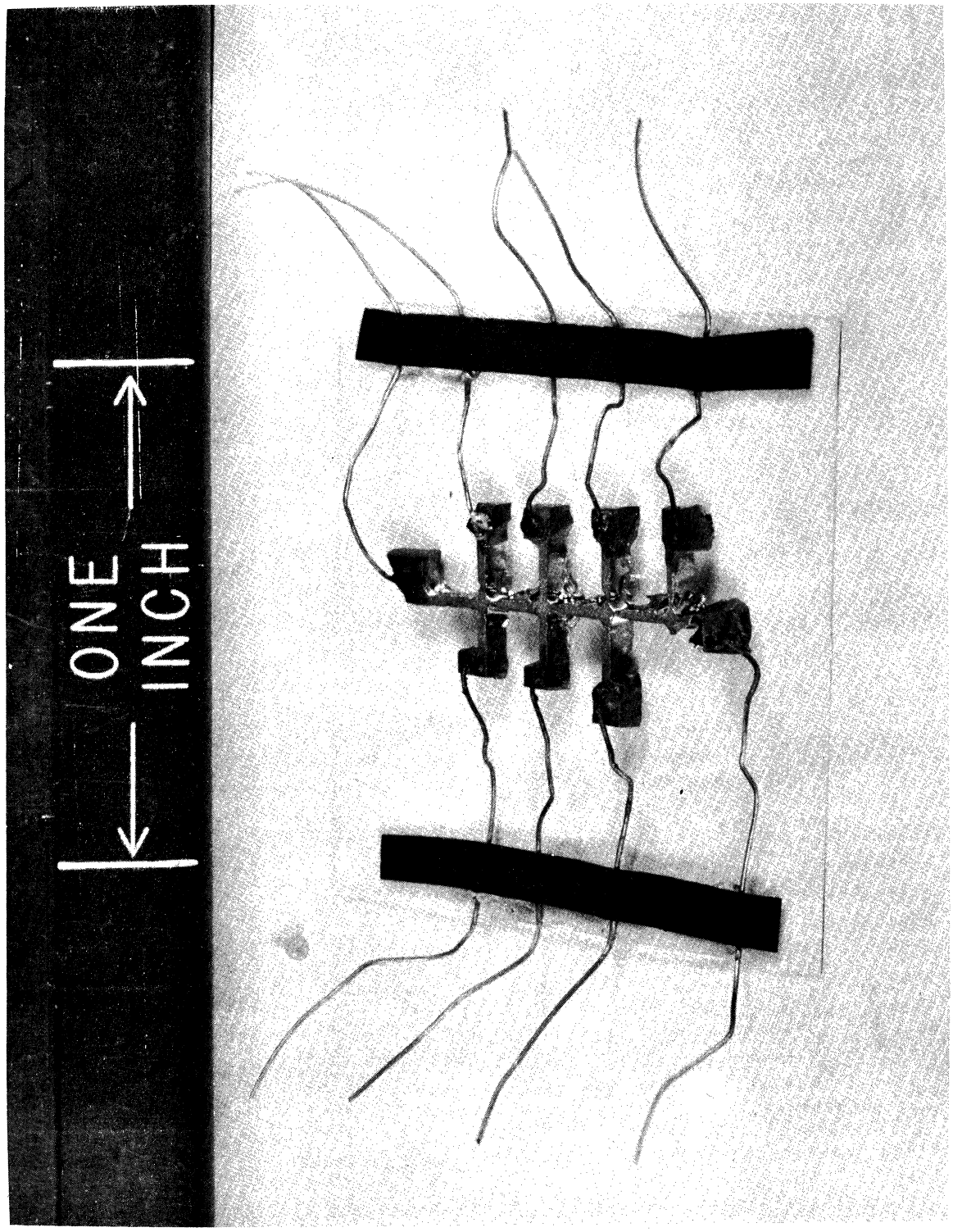

FIG. 14 SINGLE CRYSTAL SAMPLE FOR NOISE TESTS

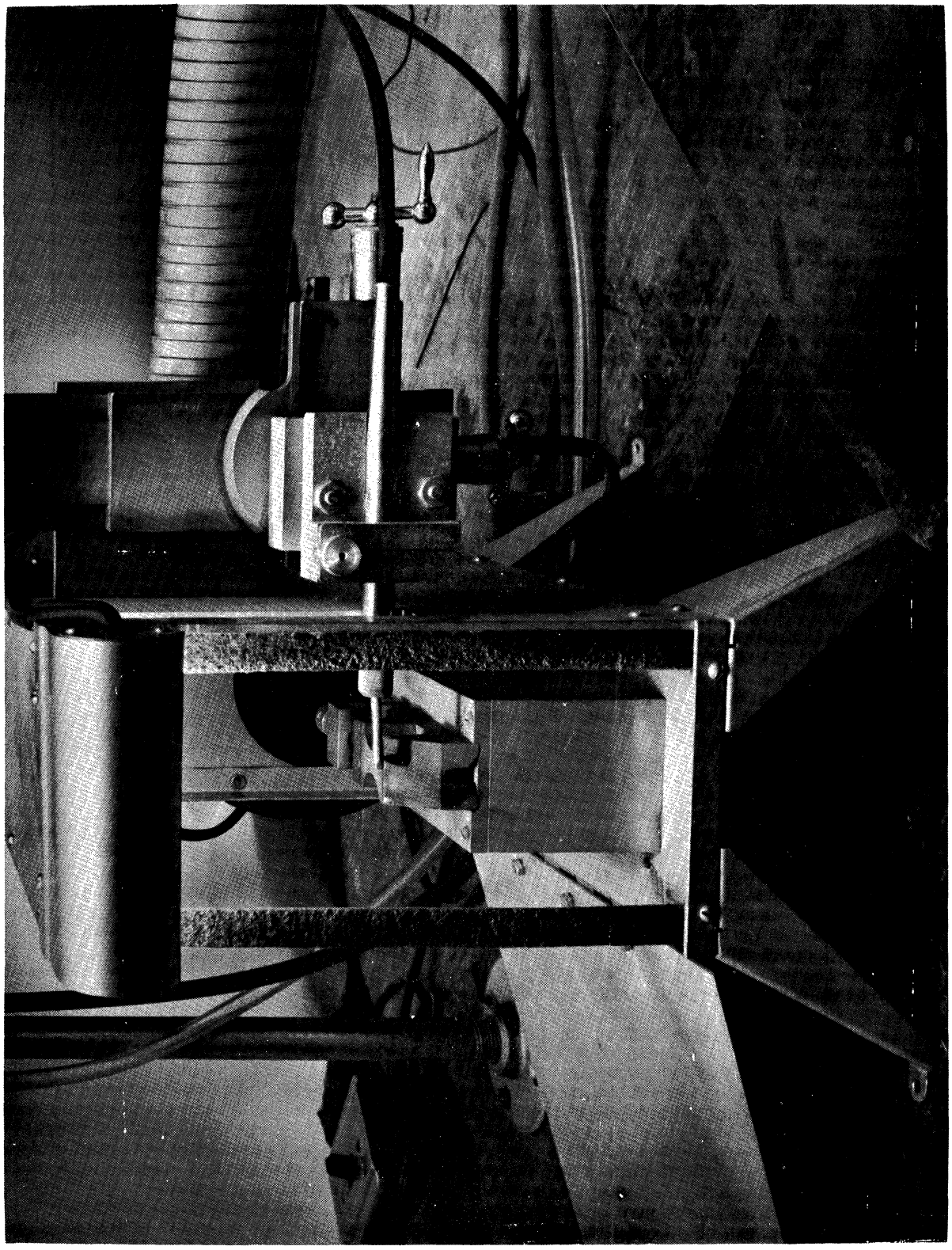

FIG. 15 DUST CUTTER

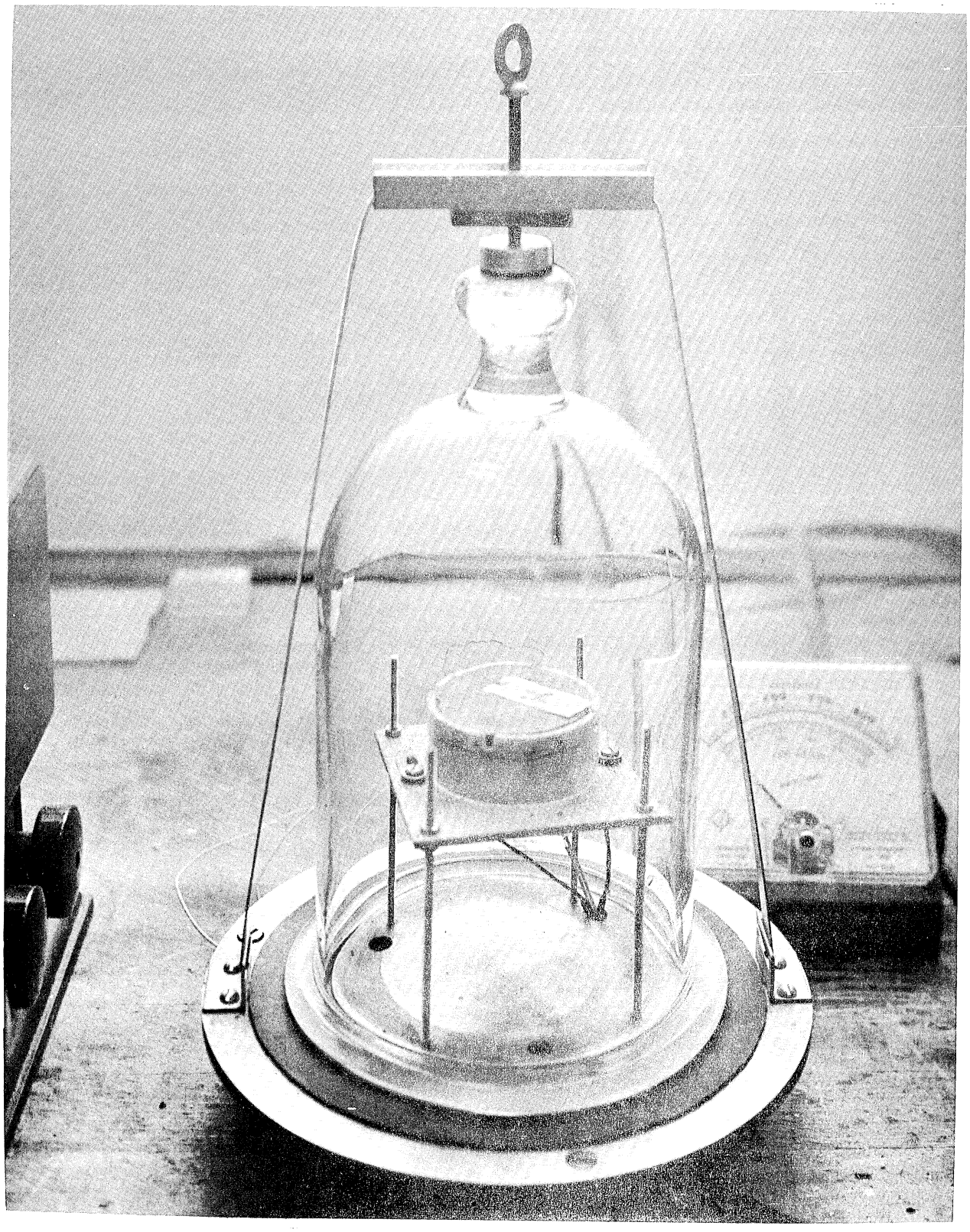

FIG. 16 HEAT TREATMENT BELL JAR

and a low-temperature cell to permit the measurement of electrical and optical properties from room temperature down to liquid-helium temperatures.

During the report period the above items, and some pieces of auxiliary equipment have been procured. The electromagnet, which will be delivered shortly, has 6-inch diameter pole pieces, with variable spacing (Varian Model V4007). The power supply is regulated with a chopper amplifier. A Leiss double monochromator has been received which, together with its additional optics, is capable of covering the spectral range from the ultraviolet to about 25 microns. An auxiliary motor drive is being constructed for use with the monochromator. An optical cell in which both optical and electrical measurements can be made at temperatures as low as that of liquid-helium has been constructed (Fig. 17). This cell is similar to one designed at the Johns Hopkins Applied Physics Laboratory (Ref. 17), but modified to permit removal of the sample holder through the bottom. A much simpler cell is being constructed for work at liquid nitrogen temperatures; the sample holders are interchangeable between the two cells.

The black-body radiator (Fig. 18) is to be used as a standard in determining and comparing the integrated spectral response of infrared detectors prepared at this and other laboratories. A design (Ref. 18) used at the Corona Laboratory of the National Bureau of Standards was adopted with some minor modifications. It consists of a heated and temperature-controlled iron cylinder containing a conical cavity, a radiation path with appropriate apertures and shields, and a radiation chopper. The chopper is driven by a synchronous motor through a pulley system by means of which chopping frequencies of 10 to 1000 cps can be obtained. The temperature is controlled by means of a MacDonald type 18A temperature controller using a platinum wire thermometer as a sensing element. Temperature is monitored by an iron-constantan thermo-couple. The iron cylinder is oxidized to give the conical cavity an effective emissivity of at least 0.99 over the range of wavelengths and temperatures of interest. This radiation source was put into operation, adjusted, and calibrated. It is capable of delivering chopped black-body radiation at temperatures ranging from ambient to 550° C.

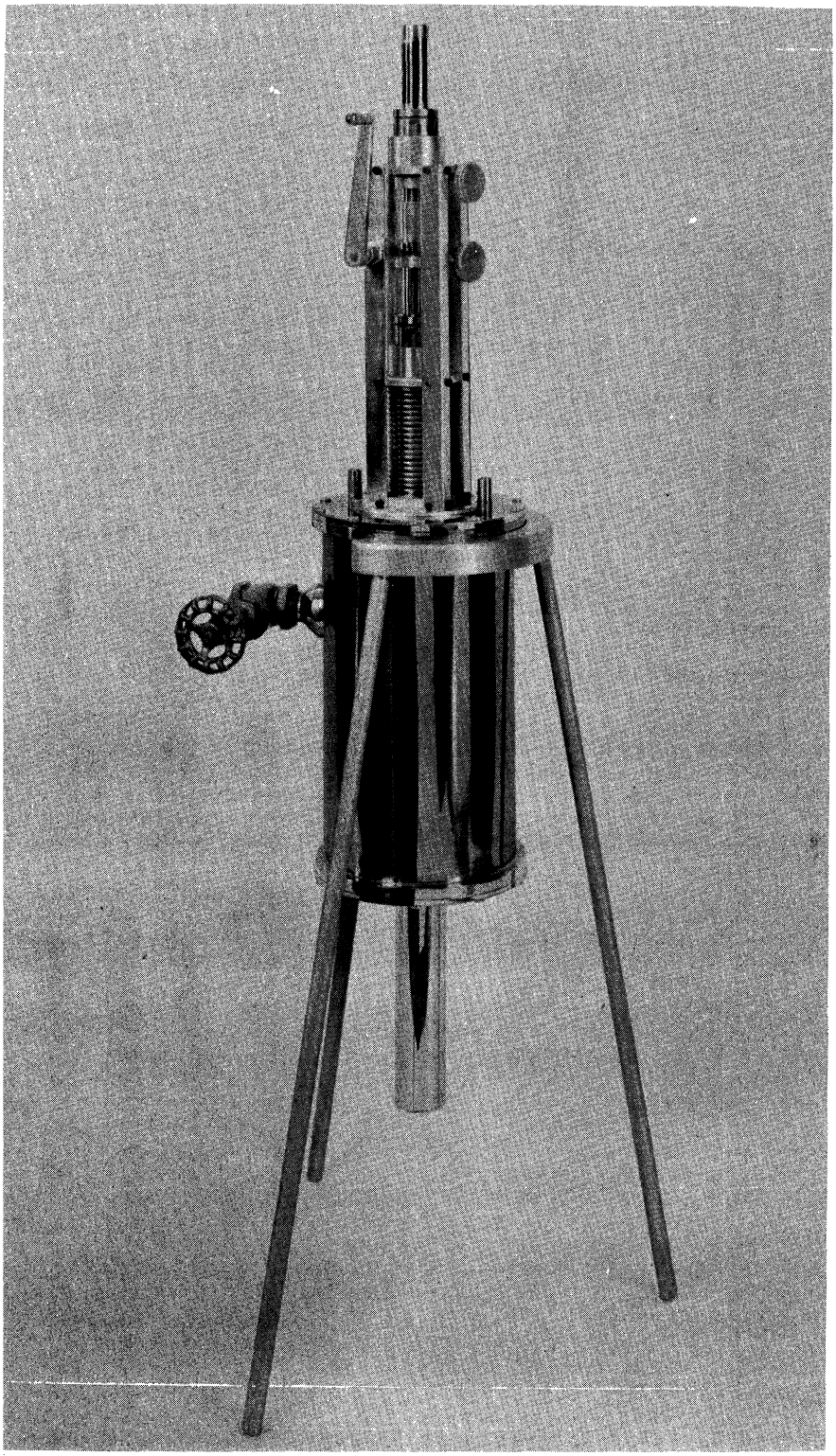

FIG. 17 CRYOSTAT

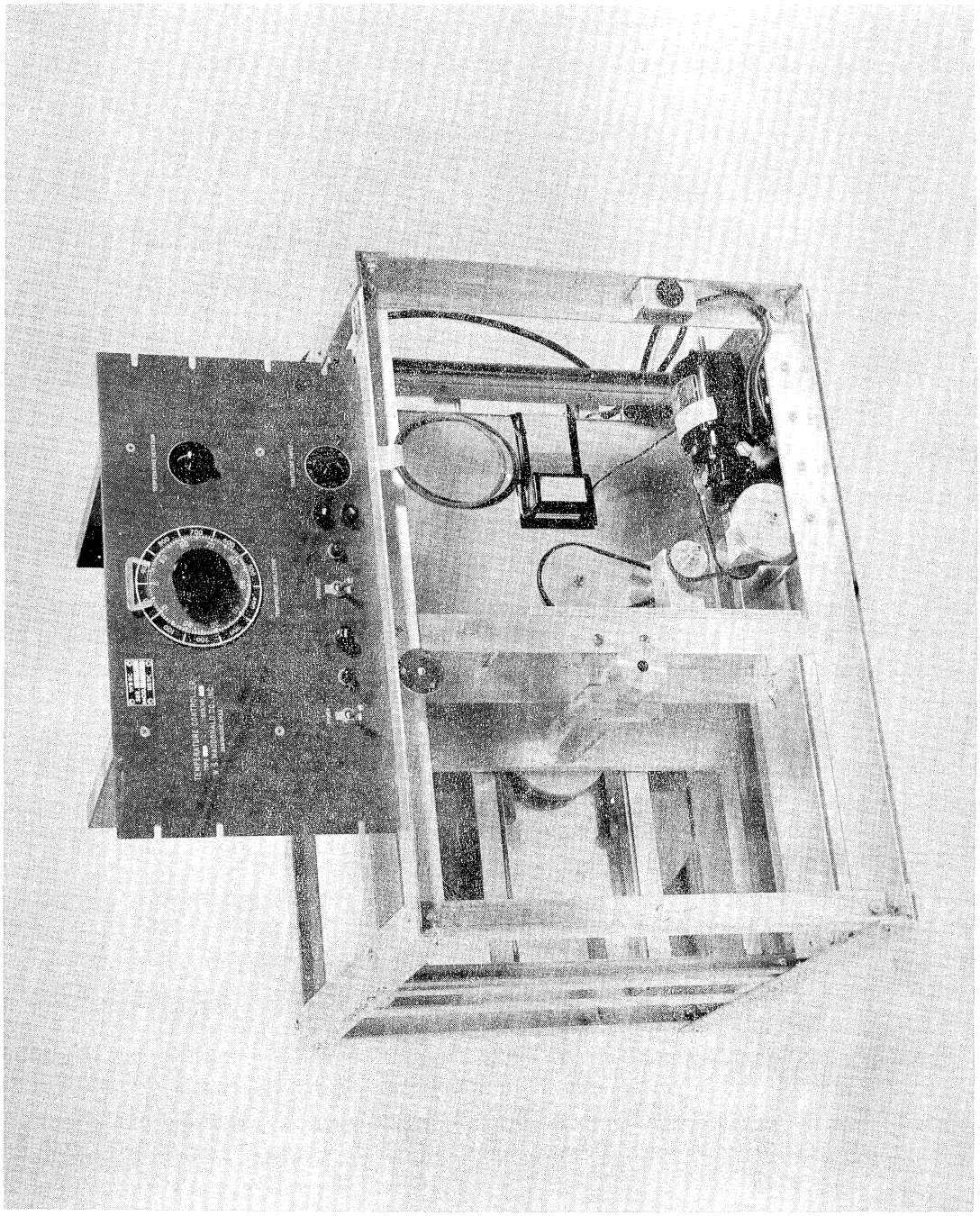

FIG. 18 BLACK BODY RADIATOR

3.2.5 Noise Studies

3.2.5.1 Theoretical Investigations

Experimental measurements have shown that noise in semiconductors varies approximately inversely with frequency, over a wide range of frequencies. A number of attempts have been made to explain the 1/f spectrum theoretically, but no single mechanism has yet been postulated which will predict the observed dependence. It has appeared attractive to some to postulate a superposition of processes (Ref. 19) whose distribution is chosen in such a way as to fit the experimental results. This has been done, for example, by van der Ziel, who used as his basic mechanism a simple recombination process (Ref. 20). He showed that the 1/f spectrum results if the probability of a given lifetime τ_p is made proportional to $1/\tau_p$, between arbitrary limits. Limits are required in order to prevent the 1/f spectrum from prevailing over all frequencies, which would imply infinite noise power. If the relationship between noise and frequency is assumed to be in the form of f^{-k}, it is necessary that k be less than unity for very low frequencies and greater than unity for very high frequencies.

During the report period the noise program has included theoretical work on noise, and instrumentation for experimental noise studies. In Appendix A, it is shown that the technique of choosing a suitable distribution function can be carried through with rather wide generality without specifying the individual microscopic process, so that it appears impossible to obtain information about any microscopic process involving such a superposition by measurements of spectral density alone. In Appendix B some relationships between spectral density and correlation function are derived, which are of significance in our current experimental noise program.

3.2.5.2 Noise Instrumentation

The initial experimental work involved instrumenting for the 0.1-cps to 15-kc region. In making the measurements the sample is mounted in a temperature-controlled holder, a suitable bias is applied, and the noise generated is observed by means of a suitable amplifier-recorder combination. A block diagram of the arrangement used is shown in Figure 19; Figure 20 shows the assembled equipment. In the following paragraphs the characteristics of the various components are discussed.

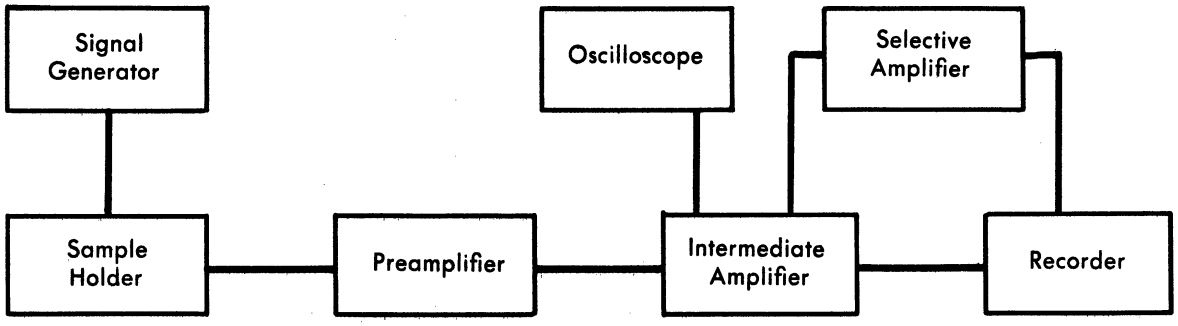

FIG. 19 BLOCK DIAGRAM OF NOISE INSTRUMENTATION

The low-temperature cell described in the previous section will be used as a sample holder in later work. However, for preliminary operation at room temperature a simple and easily accessible sample holder was built (Fig. 21). In this unit the sample is enclosed in a gas tight copper box, the temperature of which is controlled by conduction of heat down a one-half inch copper bar immersed in a constant temperature bath. The whole arrangement is insulated with styrofoam. When mounted in the holder the sample temperature variations are about 1/50 of ambient temperature fluctuations, or less than 0.1^{o} C in our location.

Preamplification was carried out by rather widely different means depending on the impedance of the sample, level of noise to be measured, and frequency at which the measurement is to be made. The noise level of the measuring system is determined by the flicker noise in the first stage of amplification. The solid curve in Figure 22 shows the measured noise equivalent resistance of our preamplifier as a function of frequency. A selected 6CB6 is being used in a cascade amplifier circuit and has given as low a noise equivalent resistance as could be expected (Ref. 21). Accurate noise measurement can only be made when the noise to be measured is at least the same order of magnitude as that obtained from the measuring equipment. Fortunately, the current noise in semiconductors increases at low frequencies at about the same rate as the flicker noise

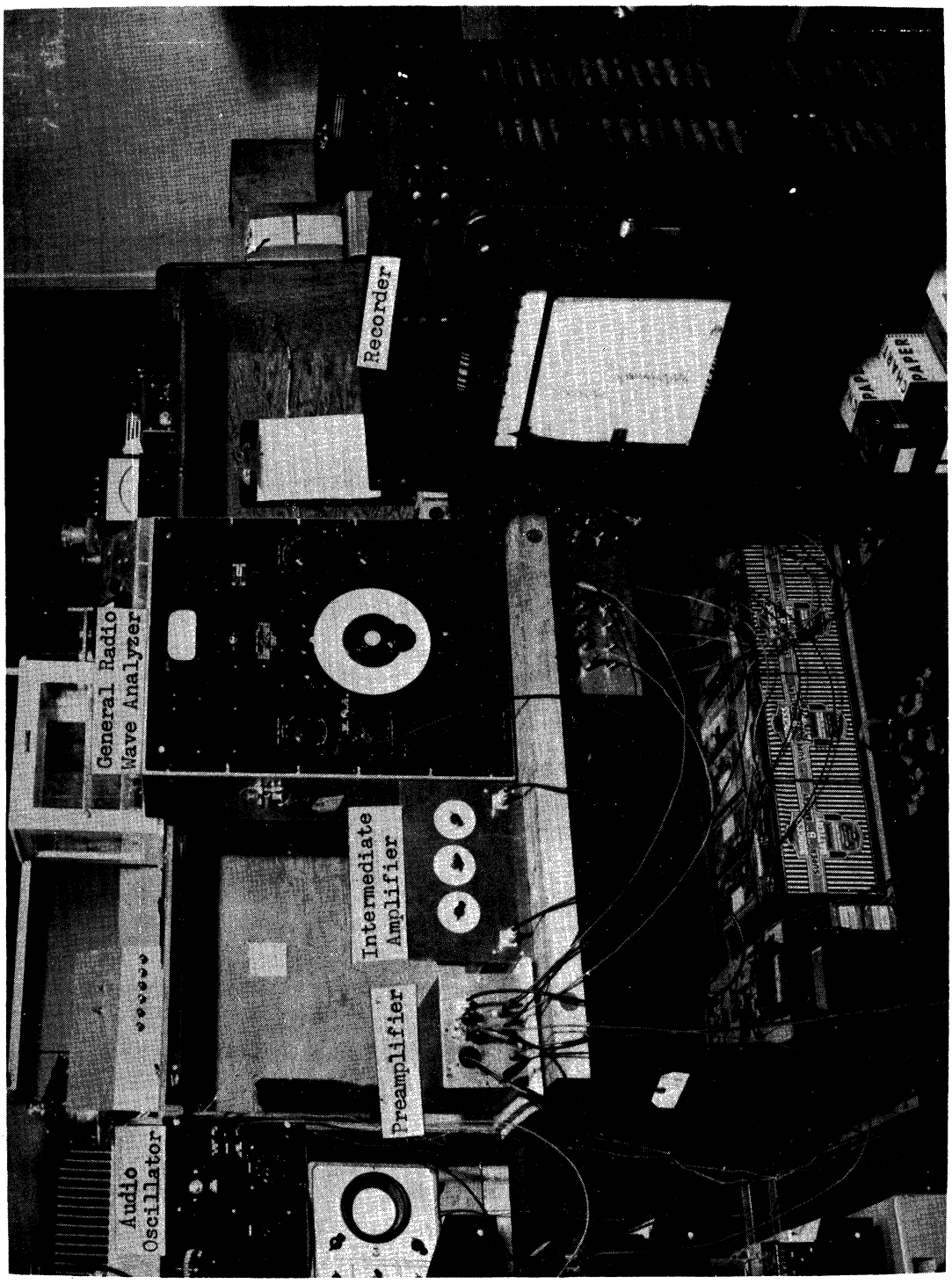

FIG. 20 NOISE MEASURING EQUIPMENT

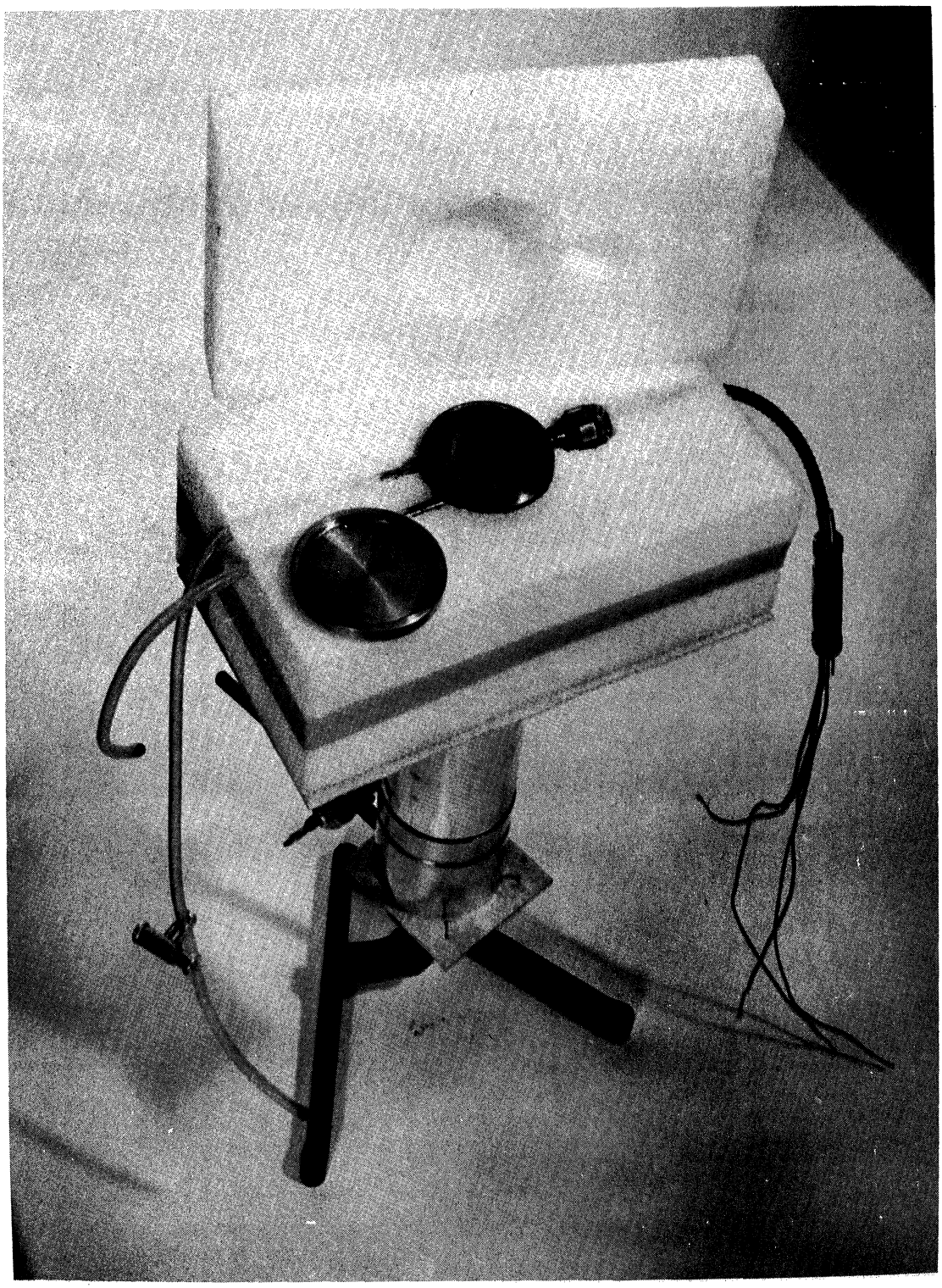

FIG. 21 SAMPLE HOLDER

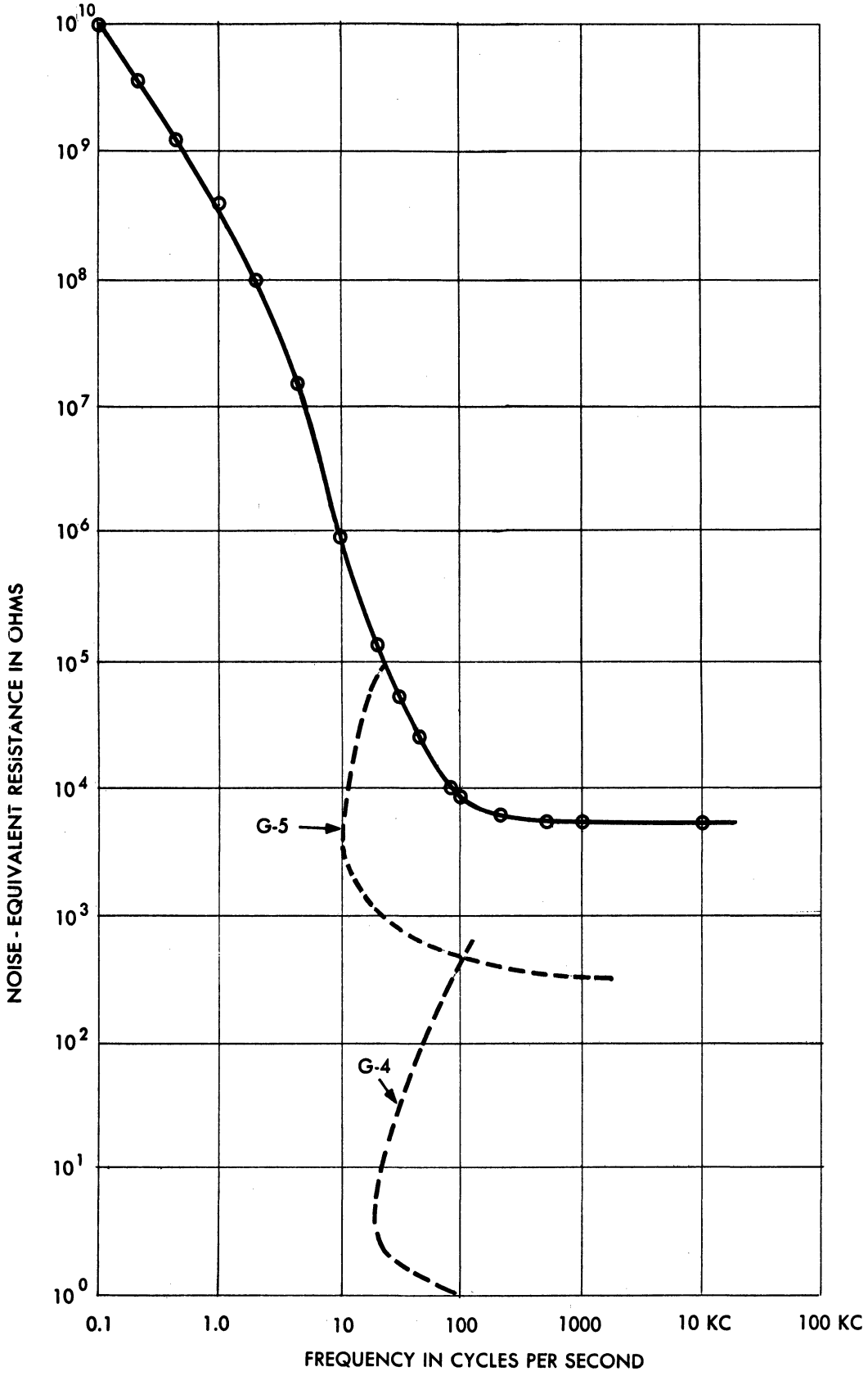

FIG. 22 NOISE EQUIVALENT RESISTANCE OF PREAMPLIFIER

in vacuum tubes. It is thus possible by direct coupling to the grid of the 6CB6 to measure at all frequencies the current noise in 0° C samples of germanium at reasonable currents if the resistance of the sample is greater than about 10,000 ohms. However, we expect a large percentage of our samples to have resistances much less than 10,000 ohms at 0° C. In order to accommodate low-resistance samples, transformers are used to obtain voltage amplification in coupling the sample to the input of the preamplifier. By this means the relative importance of amplifier noise is reduced. However the situation is more complicated by the gain of the transformer which is a function of sample resistance. The dashed curves in Figure 22 show the locus of points at which the noise from the amplifier is just equal to the Johnson noise from the sample at 0° C when using transformers G-4 and G-5 made by Triad. At greater values of frequency the situation is much more favorable. Thus with the preamplifier and the transformers it is possible to measure the current noise from 0.1 to 10 cps if the sample resistance is greater than 10,000 ohms and from 10 cps to 15 kc for samples having resistance of from one ohm to several megohms, all at 0° C. At lower temperatures all the samples will have a much greater resistance and probably about the same amount of current noise (Ref. 16). Therefore, the only additional problem expected when working at low temperature will be the reduction of the high-frequency response by the grid capacitance.

The preamplifier (without the transformer) has a voltage gain of about 2000, a frequency response which is essentially flat from 0.03 cps to 20 kc, and a cathode follower output. The preamplifier is mounted inside a double shielded copper box. Both the preamplifier and the intermediate amplifier are operated with batteries. In certain applications it is impossible to ground the sample current source. Because of pickup problems created by this it was found necessary to allow room to mount the source, a battery, and a few resistors in the preamplifier box.

The only preamplification technique which shows promise for current noise measurements below 10 cps with samples of resistance less than 10,000 ohms is the use of a chopper amplifier. In this technique, d-c or low-frequency signals are modulated on high-frequency signals before being amplified with a vacuum tube. The tube then is used as a high frequency a-c amplifier, and the effective noise equivalent resistance (due to

flicker noise) is that associated with the chopping frequency. The original low-frequency signal is restored by synchronous rectification. The Liston-Becker Model 10 AGD breaker amplifier has been tested in the 0.1 cps to 10 cps frequency range and with resistors from 5 to 10,000 ohms. The equipment noise was about 10 times Johnson noise for a resistor of 20 ohms. This is more than adequate for current noise measurements at these frequencies. However, when making current noise measurements some means of "bucking out" the d-c or a-c coupling to the amplifier is necessary. Methods of doing this are being looked into. Little emphasis is currently being placed on this very-low-frequency work.

The intermediate amplifier has a response from 0.03 cps to 20 kc, a gain of 1000, a calibrated attenuator, and variable upper and lower frequency cutoffs. A 60-cps rejection circuit, approximately 4 cycles wide at the half power points, is used to avoid saturation of later stages by 60-cps pickup, which becomes excessive when using high-impedance transformers. In addition, switching the rejection circuit in and out when measuring noise near 60 cps allows one to detect and avoid false readings due to the 60 cps.

For operation in the range 0.1 to 20 cps a selective amplifier was built. This amplifier was used to permit the measurements of noise in samples of lower resistance than was possible using the preamplifier whose characteristics are shown in Figure 22. Plug-in twin-T networks were constructed for operation at various frequencies in this range. The Q-value of the amplifier-filter combination is approximately ten at each of these frequencies. Additional passive wide-band filtering was necessary to improve the rejection characteristics of the amplifier. This unit includes a linear detector, for which the theory has been worked out (Ref. 22) and shows that the RMS value of the noise is equal to $\pi/2\sqrt{2}$ times the RMS value of a sine wave producing the same output.

The General Radio wave analyzer is used from 20 cps to 15 kc and has a constant bandwidth of approximately 4 cps. It uses a peak-reading diode detector, which behaves differently from a linear detector. The relative response to noise is dependent on the ratio of charge to discharge time. The calibration for noise was determined experimentally by measuring Johnson noise.

The relative accuracy of a noise measurement when the output from the detector is integrated is given by $(2BT)^{-1/2}$ where B is the bandwidth in cps and T is the time of the integration in seconds (Ref. 23). Thus for 1 per cent accuracy using the GR wave analyzer one has to integrate for 21 minutes. At 0.1 cps using the selective amplifier (B = 0.01 cps) one has to integrate for 21 minutes for 20 per cent accuracy, and 400 times as long for 1 per cent accuracy. When an RC circuit is used for integration about twice as much time is required for the same accuracy. It was decided, therefore, to integrate by recording and averaging using a planimeter. In order to make the averaging easier and lessen the dynamic range requirements on the recorder, an RC filter on the output of the detector with a response time around 2 per cent of the time of measurement was used. A switching arrangement was installed for adding capacitors across the meter of the GR wave analyzer giving additional time constants of 4 and 18 seconds. No change in calibration with capacity was noted. A filter of variable time constant up to 32 seconds is available for use with the selective amplifier.

The calibration signal is obtained from an audio oscillator. The output of the oscillator is measured with a vacuum thermocouple, attenuated and applied across a small resistor in series with the sample for calibration purposes. Calibration of all the equipment is performed to better than 1 per cent accuracy and noise power measurements of 5 per cent accuracy are possible.

In order to recognize interference or saturation from sources such as the radar, the arc light, and the induction furnace, it is necessary to monitor the wide-band signal with an oscilloscope.

3.2.6 One-Dimensional Lattice Calculations

A number of studies have shown that a simple one-dimensional crystal model is a valuable source of information, and can provide considerable insight into the characteristics of actual crystals. Kronig and Penney showed that such a model displays the structure of permitted and forbidden energy bands which provides the basis of theoretical explanations of semiconducting properties (Ref. 24). Saxon and Hutner studied the effects of impurities in such one-dimensional crystals, and showed how isolated

impurities add sharp energy levels in the forbidden zone, while interactions between pairs of neighboring impurities lead to split energy levels (Ref. 25). A technique developed by Ginzbarg and James makes it possible to study the effects of any arbitrary distribution of impurties (Ref. 26); they show, for example, that a random array of impurity atoms in an otherwise pure one-dimensional crystal leads to a widened band of energy levels, which may encroach upon the permitted bands of the pure material. Recently Seraphin investigated a one-dimensional representation of a 3-5 type crystal and showed that it qualitatively duplicated the observed behaviour of electron and hole mobility, forbidden energy gap, and binding energy (Ref. 27).

The results of Reference 27 are open to serious questions of interpretation which must be studied in further detail, but if correct, they suggest that the model is a far more powerful tool than had previously been suspected.

A program designed to calculate energy levels in one-dimensional crystals models was begun during the present report period. This calculation is rather complex, involving a large number of mathematical operations. Accordingly it has been programmed on MIDAC, the Michigan Digital Automatic Computer. The calculational program is designed to include an element of randomness in the crystal structure. Among the principal objectives of the program is the study of 3-5 type lattice models, including such effects as lattice disorder and impurities in their influence on physical quantities whose behaviour can be qualitatively deduced from the energy level arrangement. Our program makes use of the technique of Ginzbarg and James (Ref. 26) to study the highly important effects of random imperfections in such models. The technique consists of the following steps (for mathematical details, see Ref. 26):

1. A solution of the Schroedinger wave equation for a general cell of each type of material comprising the crystal, and for a particular assumed energy.
2. A calculation of the value and first derivative of the wave functions at the right boundary of the first cell, with specific values assigned at the left boundary.

3. A random selection of cell types in accordance with some preassigned probability rule.
4. Obtaining a continuous wave function for the entire crystal by using the calculations of (2) to match the function and first derivative at the left boundary of each cell.
5. A count of nodes in the wave function to get the number of energy levels below the assumed energy.

The procedure must be repeated for a range of energies. The wave function of (4) will not in general be an eigenfunction, but nevertheless will have the same number of nodes as the next lower eigenfunction. Each step in the above computation is relatively simple, but there are of necessity a great number of steps since a long lattice is needed to get statistical significance, and a number of energy values must be covered. Thus such a problem is well adapted to high-speed digital computation. The problem as now in operation on MIDAC uses square-well potentials, and can handle two types of materials. It is thus possible to study impurities in an otherwise pure material, or order-disorder effects in 3-5 type materials. The computation time for a 3000-atom lattice at one energy value is approximately 2.5 minutes.

Three exploratory problems have been solved to date: energy levels have been computed for a pure 3-5 type lattice, for a completely disordered mixture of the same atoms, and for a moderately disordered crystal in which there is a 90 per cent probability that a 3-type will follow a 5-type atom and vice versa. The results of these computations have not yet been analyzed in sufficient detail to report at this time.

APPENDIX A

SUPERPOSITION OF MICROSCOPIC PROCESSES

(Unclassified)

Consider an arbitrary microscopic process involving a parameter τ_p, with the restriction that the correlation function $\rho(\tau)$ can be expressed as a function of the ratio τ/τ_p:

$$\rho(\tau) = \frac{\overline{y(t)\ y(t+\tau)}}{\overline{y^2(t)}} = \rho(\tau/\tau_p) \quad . \tag{1}$$

y(t) need not be specified but for our purposes may be, for example, the fluctuating noise current through a semiconductor. By a well-known relationship (Ref. 33) the spectral density (noise power per unit frequency) is given by

$$G(f,\tau_p) = 4\overline{y^2(t,\tau_p)} \int_0^\infty \rho(\tau/\tau_p) \cos\omega\tau\, d\tau, \tag{2}$$

where $\omega = 2\pi f$. In the above equation it has been specifically indicated that both the spectral density and the average noise power, $\overline{y^2(t, \tau_p)}$, are functions of τ_p, the parameter describing the individual process. By a change of variable Equation (2) becomes,

$$G(f,\tau_p) = 4\overline{y^2(t,\tau_p)}\ \tau_p\ H(\omega\tau_p), \tag{3}$$

where for brevity we have introduced

$$H(\omega\tau_p) = \int_0^\infty \rho(x) \cos\omega\tau_p x \quad dx. \tag{4}$$

If the correlation function is exponential, H is in the form of $1/(1+\tau^2/\tau_p^2)$. If the correlation function is Gaussian in τ/τ_p (as would result, for example, if noise were produced by a process analogous to cosmic ray bursts), it can easily be shown that H is also Gaussian, in $\omega^2\tau_p^2$.

Since power is additive, the observed spectral density in the presence of a number of processes is given simply by the integral of Equation (3) over all contributing values of the parameter:

$$G(f) = \int_{\tau_p} G(f, \tau_p) d\tau_p = 4 \int_{\tau_p} \overline{y^2(t, \tau_p)}\ \tau_p\, H(\omega \tau_p)\, d\tau_p \ . \tag{5}$$

The question of "contribution" is reflected directly in the value of the average noise power, $\overline{y^2(t, \tau_p)}$, of the process.[1] It will be shown that the following distribution, with suitable choice of τ_1 and τ_2, will lead to a 1/f spectrum:

$$\begin{aligned} \overline{y^2(t, \tau_p)}\, d_p &= K\, \frac{d\tau_p}{\tau_p}\ , \quad \tau_1 < \tau_p < \tau_2 \\ &= 0\ , \quad \text{for all other } \tau_p . \end{aligned} \tag{6}$$

The introduction of Equation (6) into Equation (5) yields

$$G(f) = 4K \int_{\tau_1}^{\tau_2} H(\omega \tau_p)\, d\tau_p ; \tag{7}$$

or, by changing variables,

$$G(f) = \frac{1}{f} \cdot \frac{2K}{\pi} \int_{\omega \tau_1}^{\omega \tau_2} H(z) dz . \tag{8}$$

If the limits of integration in the above equation were zero and infinity, a 1/f spectrum would be obtained over all frequencies. However in this case the average noise power,

$$\int_{\tau_p} \overline{y^2(t, \tau_p)}\, d\tau_p = K \int_{\tau_1}^{\tau_2} \frac{d\tau_p}{\tau_p} = K \ln \frac{\tau_2}{\tau_1} , \tag{9}$$

would be infinite.

[1] This does not follow the development of Reference 33. The dependence of average noise power on $_p$ was recognized, however, in Reference 34.

In general Equation (8) is in the form of

$$G(f) = \frac{1}{f} \cdot (\text{Const.}) \tag{10}$$

provided only that

$$\int_0^\infty \rho\left(\frac{x}{\omega\tau_2}\right)\cos x\, dx - \int_0^\infty \rho\left(\frac{x}{\omega\tau_1}\right)\cos x\, dx \simeq 0. \tag{11}$$

For physically acceptable forms of correlation function (including, for example, the assumption of Gaussian bursts of noise of half-power duration τ_p), this condition is generally fulfilled if

$$\omega\tau_2 >> 1 \qquad \text{and} \qquad \omega\tau_1 << 1.$$

Since the 1/f spectrum has been observed from frequencies of fractions of a cycle to more than a megacycle, τ_1 and τ_2 must represent a range of at least 10^{-7} to 1 second.

The wide variety of microscopic processes which satisfy Equation (11) suggests that it is inherently impossible to attempt to verify a postulated process by measurements of spectral density alone.

APPENDIX B

CORRELATION FUNCTION FOR 1/f NOISE

(Unclassified)

A considerable insight into the character of the observed noise is afforded by the Fourier inversion of Equation (2). Using bars to denote averages over all processes, this is

$$\overline{y(t)\, y(t+\tau)} = \int_0^\infty \overline{G(f)} \cos 2\pi f\tau \, df. \tag{12}$$

Many workers in the field have measured $\overline{G(f)}$ for various semiconductors and related materials. Typical results show that the noise power per unit frequency in excess of Johnson noise has the form

$$G(f) = \frac{A}{1 + (2\pi f)^2 \tau_o^2} + \frac{B}{f} . \tag{13}$$

The introduction of the first term into Equation (12) leads at once to the familiar exponential correlation function of shot noise:

$$A \int_0^\infty \frac{\cos 2\pi f\tau}{1 + (2\pi f)^2 \tau_o^2} \, df = \frac{A}{4\tau_o} e^{-\tau/\tau_o} . \tag{14}$$

This term may safely be integrated from zero to infinity, even though measurements of spectral density have been made over but a limited range, since the nature of shot noise is well understood. However, in including the second term it is necessary to recognize that the frequency dependence is unknown for very high and very low frequencies. These unknown portions of the spectrum will be designated as $G_1(f)$ and $G_2(f)$, respectively:

$$\overline{y(t)\, y(t+\tau)} = \frac{A}{4\tau_o} e^{-\tau/\tau_o} + \int_o^{f_1} G_1(f) \cos\omega\tau \, df + B \int_{f_1}^{f_2} \frac{1}{f} \cos\omega\tau \, df + \int_{f_2}^{\infty} G_2(f) \cos\omega\tau \, df. \tag{15}$$

It has sometimes been stated that there are an infinite number of possible solutions to Equation (12) since G(f) is not known over the full range of frequencies. A study of Equation (15) shows that the situation is, nevertheless, not hopeless. It is found that:

1. The first integral, over $G_1(f)$, yields an inherently unknown constant, as long as $f_1\tau \ll 1$. Thus an expected reciprocity between time and frequency is found: nothing can be learned about correlation times greater than the inverse of the minimum frequency to which spectral density measurements have been made.

2. The third integral, over $G_2(f)$, is zero for allowable forms of the integrand, as long as $f_2\tau \gg 1$. This similarly sets a lower bound on the correlation times that can be considered.

The integration over the 1/f term of Equation (15) yields

$$B\int_{f_1}^{f_2} \frac{1}{f}\cos \omega\tau \, df = B\left[\ln x - \frac{x^2}{2\cdot 2!} + \frac{x^4}{4\cdot 4!} - \cdots\right]_{2\pi f_1}^{2\pi f_2} . \quad (16)$$

The requirement of (2) is that the upper limit is a large number; the limit of the series in this case is at once recognized as Euler's constant (=0.577$\cdots$). By (1) the lower limit is a small number, so that only the first term of the series need be retained. Thus, finally, consolidating all constants, it is seen that the correlation function has the form

$$\overline{y(t)\, y(t+\tau)} = \frac{A}{4\tau_o} e^{-\tau/\tau_o} - B\ln\tau + C \quad (17)$$

between limits $\tau_1 \ll 1/f_2$ and $\tau_2 \gg 1/f_1$, where f_1 and f_2 are respectively the lower and upper frequencies to which the 1/f spectrum has been detected.

The very slow decrease of the $\ln\tau$ function, arising from the 1/f spectrum, shows that significant noise correlations should be observed over long time intervals. Experiments are now being designed to use such correlations to learn something of the source and motions of the noise carriers in semiconductors (Ref. 35). Measured values of A and B (Eq. 13), when substituted in Equation (17), show the importance of knowing the relative contributions of the terms in this equation, and suggest that it may be possible to isolate the effects of the different types of noise.

REFERENCES

(Unclassified)

Number

1. 2144-12-P, "Report of Project MICHIGAN," University of Michigan, Engineering Research Institute, Willow Run Research Center (Period 1 March 1954 to 31 August 1954). SECRET

2. Louis Harris, private communication and "Preparation and Infrared Properties of Aluminum Oxide Films" by Louis Harris, J. Opt. Soc. Am. 45, 27 (1955).

3. 2144-31-R, "The Interference Edgegraph" by Vincent A. Vis, University of Michigan, Engineering Research Institute, Willow Run Research Center (January 1955). SECRET

4. "Photoconductivity in the Elements" by T.S. Moss, Academic Press, Inc., New York (1952).

5. "The Absorption Spectra of Solid Lead Sulfide, Selenide, and Telluride" by A.F. Gibson, Proc. Phys. Soc. 63B, 756 (1950).

6. Ohio AFTR-6667, "Interference Reflection Filters for Use in the Infrared Spectral Region" by R.A. Oetjen and W. H. Shaffer, Final Engineering Report on Contract W33-038ac-15400, Ohio State University Research Foundation (September 1951). RESTRICTED

7. NOL-1120, "A Method for the Determination of the Optical Constants of Semitransparent Films" by M.S. Oldham, U.S. Naval Ordnance Laboratory Report No. 1120 (31 October 1949). UNCLASSIFIED

8. "Simulator for Calculating the Reflectance and Transmittance of Multilayer Interference Films" by S.M. MacNeille and E.O. Dixon, J. Opt. Soc. Am. 44, 805 (1954).

9. "Smithsonian Physical Tables," Ninth Revised Edition prepared by W.E. Forsythe (Smithsonian Institute, Washington, D.C., 1954).

REFERENCES (Continued)

Number

10. Proceedings of the "Conference on Photoconductivity" held in Atlantic City, New Jersey, November 1954 (to be published).

11. "Uber neue halbleitende Verbindungen" by Von H. Welker, Z. Naturforschg. 7a, 744 (1952).

12. "Semiconducting Intermetallic Compounds" by R.G. Breckenridge, Phys. Rev. 90, Second Series, 488 (1953).

13. Bul. Am. Phys. Soc., 29, No. 3 (1954).

14. See, for example, the survey article by R.C. Jones, Advances in Electronics Vol. V, Academic Press, New York (1952).

15. "Principles of Zone Melting" by W.G. Pfann, J. Metals 4, 747 (1952).

16. "Electrical Noise in Semiconductors" by H.C. Montgomery, Bell System Technical Journal 31, 950 (1952).

17. "An Optical Cell for Use with Liquid Helium" by W.H. Duerig and I.L. Mador, Rev. Sci. Instr. 23, 421 (1952).

18. NBS-1225, "Procedures Used in the Study of Properties of Photoconductive Detectors" by A.J. Cussen, National Bureau of Standards, Corona, California (February 1952).

19. "A Suggestion Regarding the Spectral Density of Flicker Noise" by F.K. Dupre, Phys. Rev. 78, Second Series, 615 (1950).

20. "On the Noise Spectra of Semi-Conductor Noise and of Flicker Effect" by A.van der Zeil, Physica 16, No. 4, 359 (1950).

21. University of Minnesota - ETRL-QR-9, "Study of the Cause and Effect of Flicker Noise in Vacuum Tubes" Contract No. DA-36-039-sc-15355, University of Minnesota Institute of Technology, Electron Tube Research Laboratory (Final Report September 1953).

REFERENCES (Continued)

Number

22. "Threshold Signals" by J.L. Lawson and G.E. Uhlenbeck, Radiation Laboratory Series, Vol. 24 (McGraw-Hill Book Co., Inc., New York, 1950).

23. "Noise" by A. van der Ziel (Prentice Hall, Inc., New York 1954) p. 231.

24. "Quantum Mechanics of Electrons in Crystal Lattices" by R. de L. Kronig and W.G. Penney, Proc. Roy. Soc. 130a, 499 (1931).

25. "Some Electronic Properties of a One-Dimensional Crystal Model" by D.S. Saxon and R.A. Hutner, Philips Res. Rep. 4, 81 (1949).

26. "Band Structure in Disordered Alloys and Impurity Semiconductors" by H.M. James and A.S. Ginzbarg, J. Phys. Chem. 57, 840 (1953).

27. "Uber ein eindimensionales Modell halbleitender Verbindungen vom Typus A^{III} B^{V}" by B. Seraphin, Z. Naturforschg. 9a, 450 (1954).

28. Contract No. AF 33(600)-6175 with Servo Corporation of America

29. Contract No. AF 33(038)-3597

30. Contract No. AF 33(616)-2031

31. Contract No. AF 33(038)-25913

32. Contract No. AF 33(600)-26522

33. See, for example, "On the Theory of the Brownian Motion II" by M.C. Wang and G.E. Uhlenbeck, Rev. Mod. Phys. 17, 323 (1945).